https://doi.org/10.1093/plcell/koad090 THE PLANT CELL 2023: 1–14

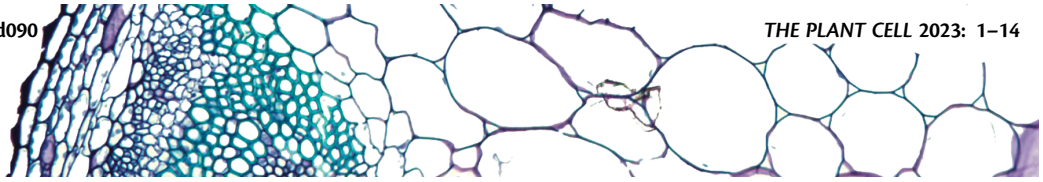

Breakthrough Report

GSK3 phosphorylates and regulates the Green Revolution protein Rht-B1b to reduce plant height in wheat

Huixue Dong [1,2,†] **Danping Li** [1,†] **Ruizhen Yang** [1] **Lichao Zhang** [1] **Yunwei Zhang** [1] **Xu Liu** [1] **Xiuying Kong** [1,*] **and Jiaqiang Sun** [1,*]

1 State Key Laboratory of Crop Gene Resources and Breeding, Institute of Crop Sciences, Chinese Academy of Agricultural Sciences, Beijing 100081, China
2 State Key Laboratory of Crop Gene Exploration and Utilization in Southwest China, Sichuan Agricultural University, Chengdu 611130, China

*Authors for correspondence: sunjiaqiang@caas.cn; kongxiuying@caas.cn.
†These authors contributed equally.
The authors responsible for distribution of materials integral to the findings presented in this article in accordance with the policy described in the Instructions for Authors (https://academic.oup.com/plcell/) are: Jiaqiang Sun (sunjiaqiang@caas.cn) and Xiuying Kong (kongxiuying@caas.cn).

Abstract

The utilization of stabilized DELLA proteins *Rht-B1b* and *Rht-D1b* was crucial for increasing wheat (*Triticum aestivum*) productivity during the Green Revolution. However, the underlying mechanisms remain to be clarified. Here, we cloned a gain-of-function allele of the GSK3/SHAGGY-like kinase-encoding gene *GSK3* by characterizing a dwarf wheat mutant. Furthermore, we determined that GSK3 interacts with and phosphorylates the Green Revolution protein Rht-B1b to promote it to reduce plant height in wheat. Specifically, phosphorylation by GSK3 may enhance the activity and stability of Rht-B1b, allowing it to inhibit the activities of its target transcription factors. Taken together, we reveal a positive regulatory mechanism for the Green Revolution protein Rht-B1b by GSK3, which might have contributed to the Green Revolution in wheat.

Introduction

During the "Green Revolution" in the 1960s, unprecedented increases in wheat yield were achieved via the introduction of the *Reduced height* (*Rht*)-*B1b* and *Rht-D1b* semidwarfing alleles to reduce plant height (Peng et al. 1999; Van De Velde et al. 2021). The gain-of-function alleles *Rht-B1b* and *Rht-D1b* encode functional DELLA proteins, which act as repressors of gibberellin (GA) signaling (Peng et al. 1999). The N-termini of DELLA proteins contain the conserved DELLA and TVHYNP motifs, which are needed for the binding of these proteins with the GA receptor GIBBERELLIN INSENSITIVE DWARF1 (GID1) (Ueguchi-Tanaka et al. 2005; Murase et al. 2008). This GID1/DELLA binding enables the DELLA protein to be recognized by the GID2/SLEEPY F-box component of an SCF ubiquitin E3 ligase, resulting in the degradation of the DELLA protein in the presence of bioactive GAs (Sasaki et al. 2003; Dill et al. 2004; Harberd et al. 2009; Hirano et al. 2010). In hexaploid wheat, DELLA proteins are encoded by 3 homoeologous *Rht-1* genes, with the wild-type alleles designated as *Rht-A1a*, *Rht-B1a*, and *Rht-D1a* (Peng et al. 1999). The *Rht-1* semidwarfing alleles resulting from a mutation in *Rht-B1a* or *Rht-D1a* are named *Rht-B1b* and *Rht-D1b* and contain a base substitution leading to a stop codon within the DELLA region (Peng et al. 1999). A recent study showed that *Rht-B1b* and *Rht-D1b* produce N-terminally truncated DELLA proteins generated by translational reinitiation, which are stabilized by the lack of an intact DELLA motif, leading to reduced plant height (Van De Velde et al. 2021).

DELLAs are destabilized not only by the canonical GID1-SCF$^{SLY1/GID2}$ pathway but also by SCF^{FKF1} and COP1 E3 ubiquitin ligases (Blanco-Tourinan et al. 2020a; Yan

Received February 1, 2023. Accepted February 25, 2023. Advance access publication March 22, 2023

IN A NUTSHELL

Background: For wheat (*Triticum aestivum*), plant height is a crucial agronomic trait because high plants are prone to lodging (falling over). During the Green Revolution in the 1960s, the unprecedented wheat yield increases were achieved through the introduction of *Reduced height* (*Rht*)-*B1b* and *Rht-D1b* semidwarfing alleles, which confer increased harvest index and improved lodging resistance. *Rht-B1b* and *Rht-D1b* alleles produce N-terminal truncated DELLA proteins generated by translational reinitiation, which are stabilized by lacking an intact DELLA motif, leading to reduced plant height. The DELLA proteins are well known as negative regulators of gibberellin signaling in plants. However, the molecular basis of how the Green Revolution proteins Rht-B1b and Rht-D1b act to reduce plant height in wheat remains to be clarified.

Question: How is the stabilized Rht-B1b protein activated or regulated to reduce plant height in wheat?

Findings: We cloned a gain-of-function allele of *GSK3* gene through characterization of a dwarf wheat mutant. The GSK3 kinase was shown to interact with and phosphorylate Rht-B1b to promote it to reduce wheat plant height. The phosphorylation by GSK3 may enhance the activity and stability of Rht-B1b. Moreover, GSK3-mediated plant growth repression requires DELLA proteins. Overall, we uncover an activation mechanism for the Green Revolution protein Rht-B1b, which not only needs to be stabilized but also needs to be activated by direct phosphorylation via GSK3 to exert its function in reducing wheat plant height.

Next steps: We plan to generate more wheat mutants with modified plant architecture by CRISPR/Cas9 or ethyl methyl sulfide (EMS) mutagenesis and elucidate the regulatory network of wheat plant architecture, which will provide new insights and elite genes for wheat improvement.

et al. 2020). In addition to ubiquitination, other posttranslational modifications, such as phosphorylation, glycosylation, and SUMOylation, also modulate the stability and activity of DELLA proteins. Rice (*Oryza sativa*) EARLY FLOWERING 1 (EL1), a homolog of the protein kinase casein kinase I (CKI), phosphorylates the N-terminal domain of the DELLA protein SLR1 to prevent its GA-mediated degradation, whereas EL1-mediated phosphorylation of its C-terminal domain sustains SLR1 activity (Dai and Xue 2010). On the other hand, Arabidopsis (*Arabidopsis thaliana*) TYPE-ONE PROTEIN PHOSPHATASE 4 (TOPP4) dephosphorylates the DELLA proteins GAI and RGA upon interaction, which is required to destabilize both DELLAs (Qin et al. 2014). In addition, the glycosylation of DELLAs adjusts their activities. For example, *O*-GlcNAcylation by SECRET AGENT (SEC) and *O*-fucosylation by SPINDLY (SPY) antagonistically modulate DELLA function: *O*-GlcNAcylation decreases the binding capacities of DELLA proteins to transcription factors (TFs), whereas *O*-fucosylation promotes the sequestration of TFs by DELLAs (Zentella et al. 2016, 2017; Blanco-Tourinan et al. 2020b). The modification of DELLAs via SUMOylation also appears to modulate their activity and stability under stress conditions (Conti et al. 2014; Blanco-Tourinan et al. 2020b).

Brassinosteroid (BR) is another important growth-promoting phytohormone that regulates some key agronomic traits, including plant height, leaf angle, grain size, and tillering (Tong and Chu 2018). BRI1-EMS SUPPRESSOR1 (BES1) and BRASSINAZOLE-RESISTANT1 (BZR1) are master TFs of BR signaling that control BR-regulated gene expression (He et al. 2002; Wang et al. 2002; Yin et al. 2002; Yu et al. 2011). The GSK3/SHAGGY-like kinase BRASSINOSTEROID INSENSITIVE 2 (BIN2) and its homologs are crucial negative regulators of BR signaling, which inactivate BES1 and BZR1 by direct phosphorylation (Li et al. 2001; He et al. 2002; Li and Nam 2002; Yin et al. 2002).

In this study, we cloned a gain-of-function allele of *GSK3* by characterizing a dwarf wheat mutant. Importantly, we found that the GSK3/SHAGGY-like kinase GSK3 phosphorylates and promotes the Green Revolution protein Rht-B1b to reduce plant height. Furthermore, we show that phosphorylation by GSK3 helps Rht-B1b repress the activities of downstream TFs that regulate plant height. Therefore, we uncovered a positive regulation mechanism for the Green Revolution protein Rht-B1b via GSK3-mediated phosphorylation.

Results

Cloning of the *GSK3* gene

In a screening for regulators of plant architecture in wheat, we identified a dwarf mutant named *gsk3* (see gene cloning information below) from an ethyl methyl sulfide (EMS) mutant library in the wheat cultivar YZ4110 background (Figs. 1A and S1, A and C). Compared with YZ4110, both the internode length and cell length were reduced and the grains were semispherical in the *gsk3* mutant (Supplemental Fig. S1, D and F). Moreover, the *gsk3* mutant was insensitive to exogenous BR treatment in both leaf angle and primary root elongation assays (Supplemental Fig. S2), suggesting that BR signaling might be affected in the *gsk3* mutant. Genetic analysis of a BC_4F_2 population from a cross between the *gsk3* mutant and YZ4110 indicated that the dwarf phenotype of *gsk3* was caused by a semidominant mutation in a single gene (Supplemental Fig. S3A; $\chi^2 = 5.31 < \chi^2_{0.05} = 5.99$).

Bulked segregant analysis-based exome capture sequencing (BSE-Seq) analysis using the BC_4F_2 population showed that *TraesCS3D02G137200* is a candidate gene located on chromosome 3D, in which 1 SNP (G/A) was identified (Supplemental Fig. S3, B and C). *TraesCS3D02G137200* encodes a GSK3/SHAGGY-like kinase, the homolog of the Arabidopsis BR signaling component BIN2 (Supplemental Fig. S4), which interacts with TaBSU1, the homolog of the Arabidopsis BIN2 regulator BSU1 (Supplemental Fig. S5). The G to A mutation changes the conserved $TREE^{286}$ domain of GSK3 to $TREK^{286}$ in the *gsk3* mutant (Supplemental Fig. S4). *gsk3-Flag* transgenic lines displayed obviously reduced plant height compared with *GSK3-Flag* transgenic lines and wild-type KN199 (Supplemental Fig. S3, D and E). Immunoblotting demonstrated that the Glu286Lys point mutation enhances the protein stability of gsk3 (Supplemental Fig. S3, F and G). Similarly, the $GSK3^{E285K}$*-Flag* transgenic wheat plants also displayed a dwarf phenotype (Fig. 1B). In support of our view, two independent studies demonstrated that the natural mutation Glu286Lys in GSK3 from Indian dwarf wheat (*Triticum sphaerococcum* Perc.) causes dwarf and semispherical grain phenotypes (Cheng et al. 2020; Gupta et al. 2021). Therefore, we cloned the *GSK3* gene by characterizing a dwarf wheat mutant.

GSK3 interacts with the Green Revolution protein Rht-B1b

To explore whether GSK3 is related to the Green Revolution in wheat by reducing plant height, we tested the interaction of GSK3 and Rht-1. Yeast 2-hybrid (Y2H) assays showed that GSK3 could interact with both wild-type DELLA protein Rht-B1a and truncated DELLA protein Rht-B1b (Fig. 1C). Firefly luciferase complementation imaging (LCI) assays in *Nicotiana benthamiana* leaves revealed interaction signals in samples co-expressing nLUC-GSK3/cLUC-Rht1-B1b, whereas no signal was detected in the negative controls (Fig. 1D). Pull-down assays showed that Rht1-B1b-GST (but not GST alone) pulled down MBP-GSK3 protein (Fig. 1E), demonstrating that GSK3 directly interacts with Rht1-B1b *in vitro*. Finally, co-immunoprecipitation (Co-IP) assays verified that GSK3 interacts with Rht1-B1b *in vivo* (Fig. 1F). Taken together, these observations demonstrate that wheat GSK3 interacts with the Green Revolution protein Rht1-B1b.

To comprehensively evaluate the different regions of Rht-1 protein responsible for the interaction with GSK3, we performed LCI assays in *N. benthamiana* leaves using truncated versions of the full-length Rht-1 protein Rht-B1a instead of Rht-B1b. The N-terminus but not the C-terminus of Rht-B1a interacted with GSK3 (Fig. 1G). The deletion of either the DELLA or TVHYNP motif did not affect the interaction between Rht-B1a and GSK3 (Fig. 1G), suggesting that the DELLA and TVHYNP motifs are not responsible for the interaction of Rht-B1a with GSK3. Finally, we demonstrated that the middle region of Rht-B1a, which is also present in Rht-B1b, mediates the interaction with GSK3 (Fig. 1G).

GSK3 phosphorylates Rht-B1b

Since GSK3 is a serine/threonine kinase, we wondered whether GSK3 can phosphorylate the Rht-1 proteins. To this end, we used a Phos-tag approach by incubating the MBP-GSK3 and Rht-B1a-GST proteins in kinase reaction buffer. As shown in Fig. 2A, only incubation with MBP-GSK3 and ATP generated a slowly migrating band of Rht-B1a protein in a Phos-tag gel, indicating that Rht-B1a could be phosphorylated by the GSK3 kinase. Given that the N-terminus of Rht-B1a mediates the interaction with GSK3, we speculated that the phosphorylation sites of GSK3 might be located in the N-terminus of Rht-B1a. We analyzed the putative GSK3 phosphorylation motifs (Ser/Thr-X-X-X-Ser/Thr; Wang et al. 2002; Youn and Kim 2015) in the N-terminal region of Rht-B1a. We mutated all the putative phosphorylation Ser/Thr sites in these motifs to Ala (mimic nonphosphorylated form) and performed *in vitro* phosphorylation assays with the mutant Rht-B1a protein. However, this mutant Rht-B1a protein could also be phosphorylated by GSK3 (Fig. 2A).

Thus, we mutated the remaining serine residues of the N-terminus of Rht-B1a in 2 groups (m1 and m2) (Fig. 2B). In *in vitro* phosphorylation assays, $Rht\text{-}B1a^{m1}$ mutant protein could still be phosphorylated by GSK3, whereas $Rht\text{-}B1a^{m2}$ mutant protein was barely phosphorylated by GSK3 (Fig. 2C), indicating that the phosphorylation sites are included in m2. Furthermore, $Rht\text{-}B1a^{S158A/S201A/S202A}$ mutant protein could not be phosphorylated by GSK3 (Fig. 2D), suggesting that the Ser158, Ser201, and Ser202 residues of Rht-B1a are GSK3 phosphorylation sites. As expected, GSK3 could phosphorylate Rht-B1b but not $Rht\text{-}B1b^{S92A/S135A/S136A}$, whose mutations corresponded to those of $Rht\text{-}B1a^{S158A/S201A/S202A}$ (Figs. 2E and S6). Simultaneously, the Ser135 and Ser136 residues of Rht-B1b were also identified as putative phosphorylation sites in mass spectrometry assay using Rht-B1b-GST protein (Figs. 2F and S7). Moreover, $Rht\text{-}B1b^{S92A/S135A/S136A}$ ($Rht\text{-}B1b^{3A}$) still interacted with GSK3, as did Rht-B1b, excluding the possibility that these mutations indirectly affect the phosphorylation of Rht-B1b by impairing its interaction with GSK3 (Fig. 2, G and H). In conclusion, our results demonstrate that GSK3 can phosphorylate the Green Revolution protein Rht-B1b.

GSK3 phosphorylates Rht-B1b to reduce plant height

During the Green Revolution in wheat, the Rht-B1b protein (which was generated from Rht-B1a) became stabilized and caused a semidwarfing phenotype. However, the molecular basis for the role of Rht-B1b in reducing plant height remains to be clarified. To evaluate the role of Rht-B1b phosphorylation by GSK3 in reducing plant height, we generated *Rht-B1b-OE* and $Rht\text{-}B1b^{3A}$*-OE* ($Rht\text{-}B1b^{S92A/S135A/S136A}$*-OE*) transgenic wheat plants overexpressing these genes under

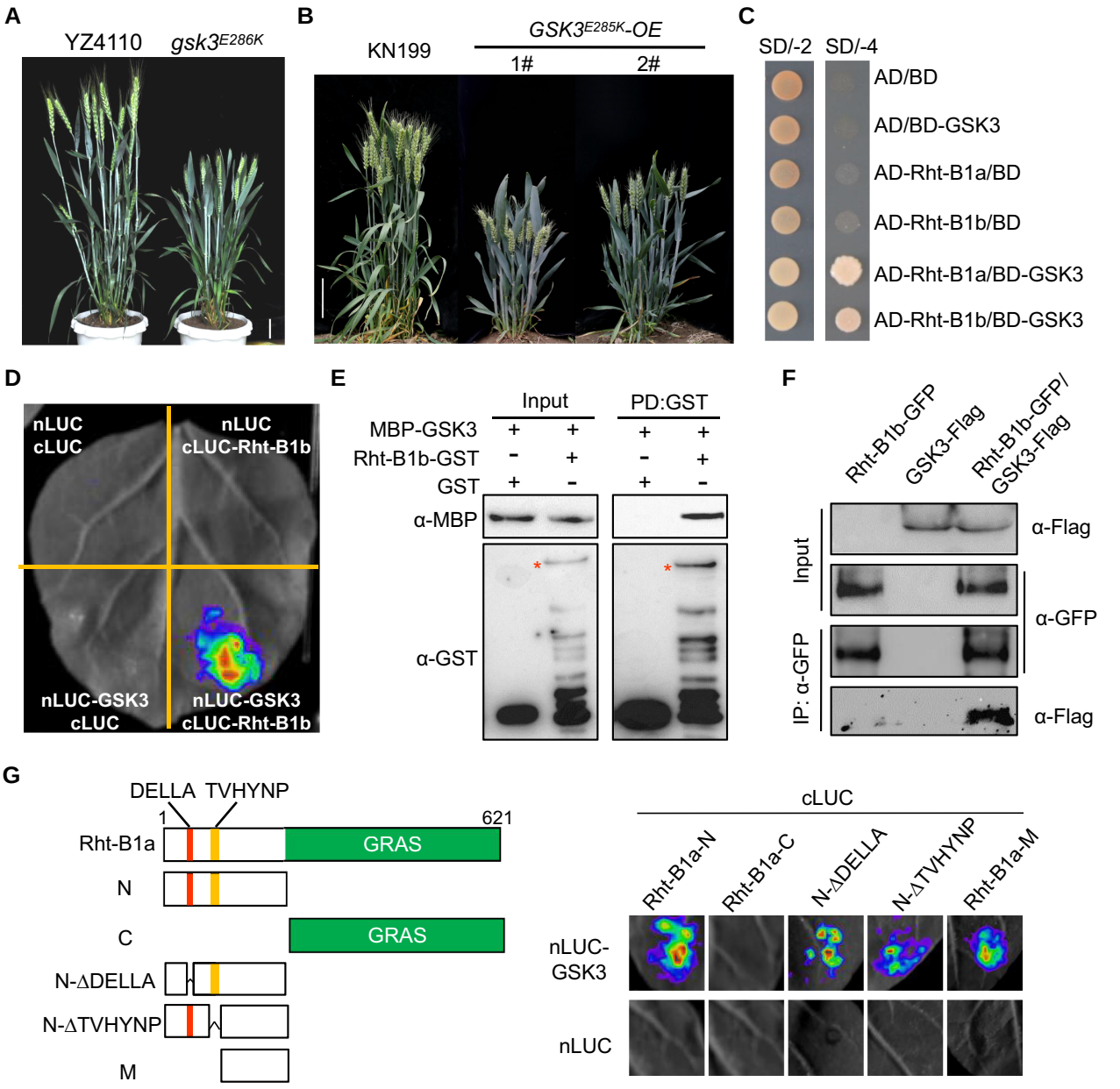

Figure 1. Gain-of-function mutations of *GSK3* reduce plant height, and GSK3 interacts with the Green Revolution protein Rht-B1b in wheat. **A)** Reduced plant height of the gain-of-function mutant *gsk3* at the heading stage compared with the wild type (YZ4110). Scale bar, 5 cm. **B)** Reduced plant height of *GSK3*^{E285K} transgenic plants compared with the wild type (KN199). Scale bar, 10 cm. **C)** Y2H assay showing that GSK3 interacts with Rht-1. SD/-2, SD-Trp/-Leu; SD-4, SD-Trp/-Leu/-His/-Ade. **D)** LCI assay showing the interaction between GSK3 and Rht-B1b. Empty vectors were used as negative controls. **E)** Pull-down assay showing that GSK3 interacts with Rht-B1b in vitro. Purified MBP-GSK3 proteins could be pulled down by Rht-B1b-GST proteins. GST was used as a negative control. Anti-MBP and anti-GST antibodies were used for immunoblotting. PD, pull down. Asterisks indicate the specific bands. **F)** Co-IP assay showing that GSK3 interacts with Rht-B1b in vivo. Rht-B1b-GFP was co-expressed with GSK3-Flag in *N. benthamiana* leaves. Protein extracts were immunoprecipitated with anti-GFP antibody. Immunoblots were probed with anti-GFP and anti-Flag antibodies. **G)** LCI assay showing that the middle region (aa 109 to 223) of Rht-B1a mediates the interaction with GSK3. Rht-B1a-N, aa 1 to 223; N-ΔDELLA, Rht-B1a-N lacking the DELLA motif (DELLA, aa 40 to 50); N-ΔTVHYNP, Rht-B1a-N lacking the TVHYNP motif (TVHYNP, aa 92 to 108); Rht-B1a-M, aa 109 to 223; Rht-B1a-C, aa 224 to 621.

control of the *Ubiquitin* promoter. Phenotypic analyses showed that most but not all *Rht-B1b-OE* transgenic plants displayed severely reduced plant height, while selected *Rht-B1b*^{3A}*-OE* transgenic plants with roughly similar expression levels of the transgene displayed a semidwarf phenotype compared with wild-type Fielder (Fig. 3, A and B and Supplemental Table S1). Moreover, overexpression of Rht-B1b severely repressed coleoptile growth, while Rht-B1b^{3A} had a minor effect on repressing coleoptile growth (Fig. 3, C and D).

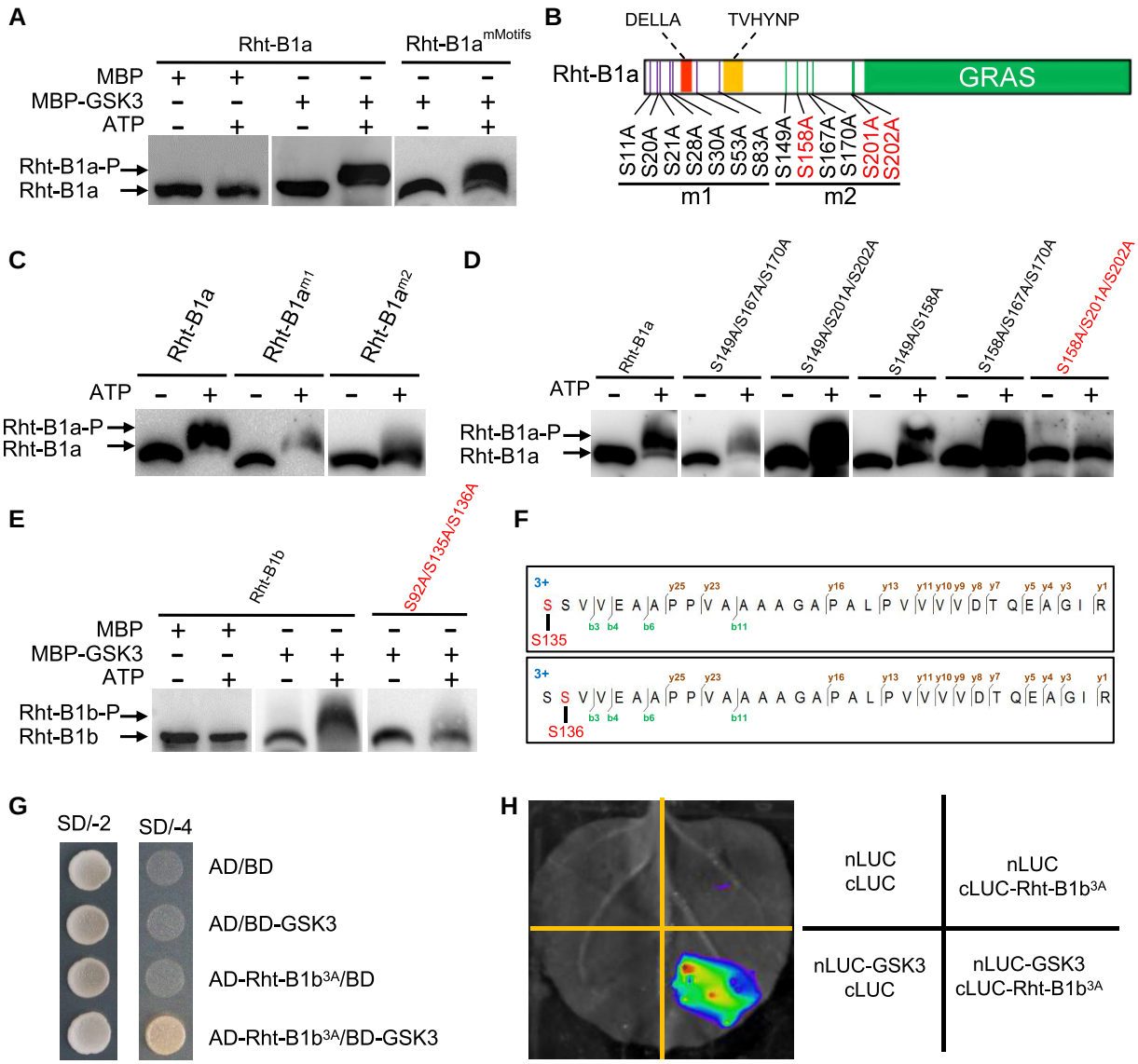

Figure 2. Rht-B1b is phosphorylated by GSK3. **A)** Protein phosphorylation assays of Rht-B1a by GSK3 using Phos-tag gel. The mutated sites of Rht-B1a^{mMotifs} are Ser/Thr residues in the putative motifs recognized by GSK3 kinase located in the N-terminal region of Rht-B1a. **B)** Schematic representation of the potential phosphorylation sites of Rht-B1a protein by GSK3. Numbers indicate the positions of amino acid residues in Rht-B1a. **C)** Protein phosphorylation assays of Rht-B1a by GSK3 using Phos-tag gel. The mutated sites of Rht-B1a^{m1} and Rht-B1a^{m2} are shown in **B)**. **D**) Protein phosphorylation assays showing that the Ser158, Ser201, and Ser202 residues of Rht-B1a are the phosphorylation sites by GSK3. **E)** Protein phosphorylation assays showing that the Ser92, Ser135, and Ser136 residues of Rht-B1b are the phosphorylation sites by GSK3. The Ser92, Ser135, and Ser136 residues of Rht-B1b correspond to the Ser158, Ser201, and Ser202 residues of Rht-B1a, respectively. In **A)** and **C** to **E)**, MBP-GSK3 proteins were incubated with different mutant forms of Rht-1-GST. Proteins were detected by immunoblotting with anti-GST antibody. Arrows indicate the phosphorylated or nonphosphorylated protein bands. **F)** The phosphorylated peptides of Rht-B1b determined by LC-MS/MS. The putative phosphorylation residues are marked in red. **G)** Y2H assay showing that GSK3 interacts with Rht-B1b^{3A}. SD/-2, SD-Trp/-Leu; SD-4, SD-Trp/-Leu/-His/-Ade. **H)** LCI assay showing that GSK3 interacts with Rht-B1b^{3A}. Empty vectors were used as negative controls. The red texts in this figure refer to putative phosphorylation residues of Rht-B1a or Rht-B1b.

Reverse transcription quantitative PCR (RT-qPCR) and immunoblotting assays confirmed that the levels of Rht-B1b were roughly similar in these transgenic lines (Fig. 3, E and F). Furthermore, we performed *in vivo* phosphorylation assays of Rht-B1b using stably transgenic wheat plants. An upshift of the phosphorylated band of Rht-B1b from *Rht-B1b-OE* plants was observed in the Phos-tag gel (Fig. 3G). However, the phosphorylated band of Rht-B1b^{3A} was undetectable from *Rht-B1b^{3A}-OE* plants (Fig. 3G). Taken together, these results demonstrate that phosphorylation by GSK3 facilitates the activity of Rht-B1b, allowing it to reduce plant height in wheat.

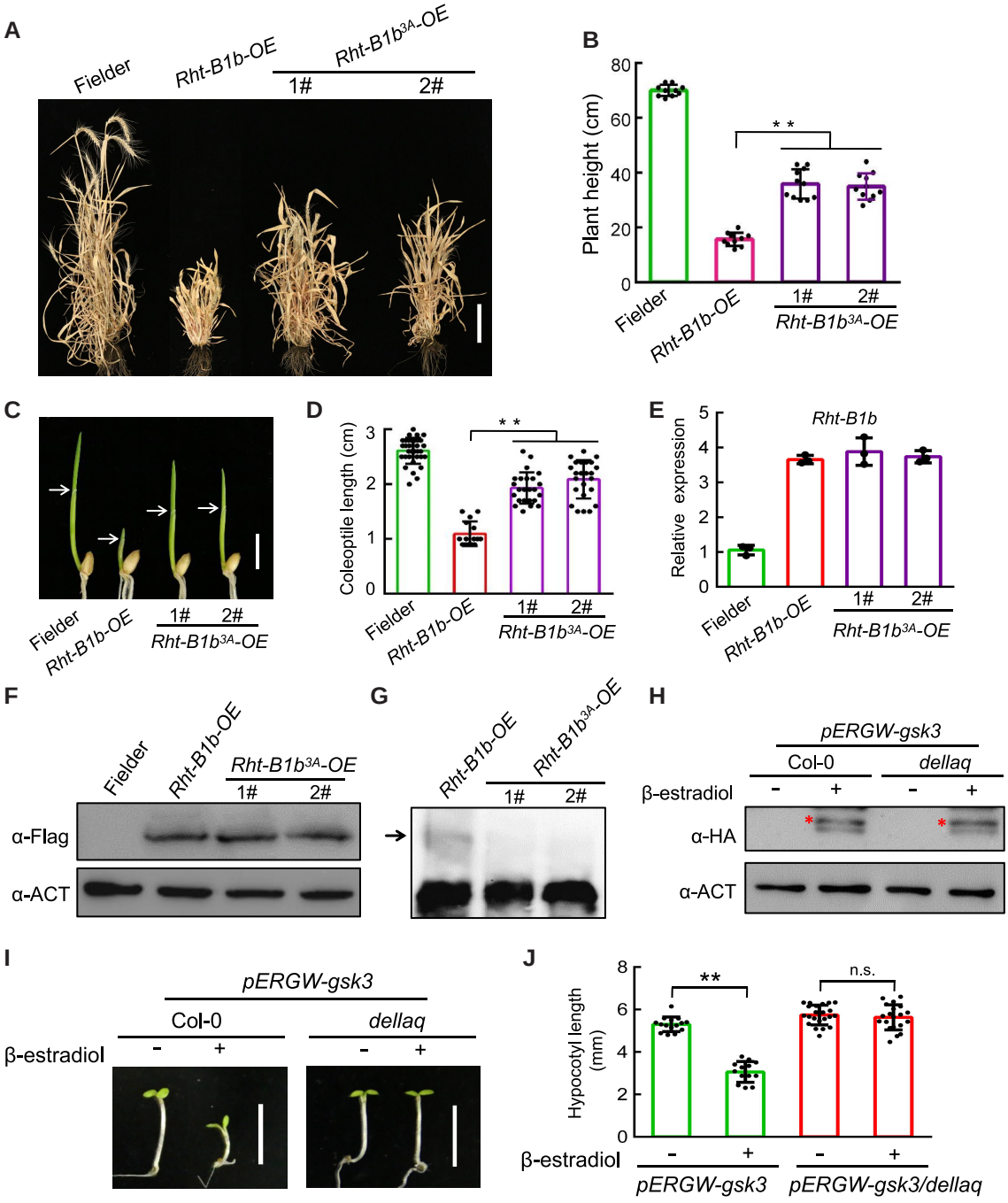

Figure 3. Rht-B1b reduces plant height with the assistance of GSK3. **A)** Plant heights of representative *Rht-B1b-OE* and *Rht-B1b*^{3A}*-OE* transgenic plants. Rht-B1b^{S92A,S135A,S136A} is labeled as Rht-B1b^{3A}. Scale bar, 20 cm. **B)** Quantification of plant height of representative transgenic plants at the mature stage. Error bars represent means ± SD ($n \geq 10$). Asterisks indicate significant differences by Student's *t* test (**$P < 0.01$). **C, D)** The phosphorylation of Rht-B1b is required to repress coleoptile growth in wheat. The image in **C)** shows the coleoptile phenotypes of representative transgenic plants. Scale bars, 10 mm. The quantification of coleoptile lengths is shown in **D)**. Error bars denote ± SD ($n > 18$). **$P < 0.01$, Student's *t* test. **E, F)** Transcriptional and protein level analyses of Rht-B1b in representative transgenic plants. The transcript levels of *Rht-B1b* were quantified by normalizing against *TaGAPDH*, and values represent means ± SD ($n = 3$). Actin was used as a loading control. **G)** Phosphorylation assays showing that the phosphorylation of Rht-B1b^{3A} was affected *in vivo*. Proteins were extracted from the *Rht-B1b-Flag* and *Rht-B1b*^{3A}*-Flag* transgenic wheat plants and separated on the Phos-tag gel. Anti-Flag antibody was used to detect the Rht-B1b proteins. **H)** Inducible protein accumulation analysis of gsk3 in the indicated Arabidopsis backgrounds. The seedlings were treated without or with 10 μM β-estradiol for 6 h. Anti-HA antibody was used to detect the gsk3 protein levels, and actin was used as a loading control. Asterisks indicate specific protein bands. **I, J)** Plant growth phenotypes of *pERGW-gsk3*/Col-0 and *pERGW-gsk3/dellaq* transgenic Arabidopsis plants. Seedlings were grown on 1/2 MS medium without or with 10 μM β-estradiol for 6 d. Error bars represent means ± SD ($n \geq 15$). Asterisks indicate significant differences, and n.s. indicates no significant difference by Student's *t* test (**$P < 0.01$).

GSK3-mediated growth repression genetically requires DELLA proteins

To determine whether GSK3-mediated growth repression is related to DELLA proteins, we generated transgenic plants harboring *pERGW-gsk3* (expressing *gsk3* driven by a β-estradiol–inducible promoter) in the Arabidopsis Col-0 and *dellaq* quadruple mutant (*gai-t6 rga-t2 rgl1-1 rgl2-1*; Achard et al. 2007) backgrounds. As shown in Fig. 3H, gsk3 levels were similar in Col-0 and *dellaq*. In the absence of the inducer β-estradiol, the hypocotyls of *pERGW-gsk3*/*dellaq* were significantly longer than those of *pERGW-gsk3*/Col-0 grown under normal light conditions (Supplemental Fig. S8A).

To easily observe the repressive effect of gsk3 on hypocotyl elongation, we grew these transgenic seedlings under weak light conditions. The plants displayed comparable hypocotyl lengths (Fig. 3, I and J). In the presence of the inducer β-estradiol, the induction of gsk3 dramatically repressed hypocotyl elongation in Col-0 but not in the *dellaq* mutant background (Fig. 3, I and J), suggesting that GSK3-mediated growth repression requires the functions of DELLA proteins. As expected, the induction of gsk3 caused a BR-insensitive phenotype in both the WT and *dellaq* backgrounds (Supplemental Fig. S8B). However, gsk3-induced transgenic plants in the WT background could still respond to GA to some extent, whereas those in the *dellaq* background were insensitive to GA (Supplemental Fig. S8C). These results suggest that GA-induced destruction of DELLA proteins may be predominant over the enhancement of DELLA function by GSK3.

Phosphorylation facilitates Rht-B1b–mediated inhibition of target TF activity

Studies in Arabidopsis showed that DELLA proteins exert their function by suppressing the DNA-binding activities of PHYTOCHROME-INTERACTING FACTOR (PIF) family TFs on the target genes (de Lucas et al. 2008; Feng et al. 2008). To evaluate the role of phosphorylation by GSK3 on Rht-B1b function, we confirmed the physical interaction between Rht-B1b and PIF4. Pull-down assays showed that Rht-B1b-GST proteins directly interact with MBP-PIF4 proteins *in vitro* (Fig. 4A). We recently reported that TaPIL1, a wheat homolog of Arabidopsis PIF4, positively regulates plant height (Zhang et al. 2022). LCI assays demonstrated that Rht-B1b and Rht-B1b^{3A} interacted with PIF4/TaPIL1 in a similar manner (Fig. 4, B and C), excluding the possibility that the mutations of Rht-B1b^{3A} affect its activity by impairing protein folding.

Furthermore, we employed the well-documented PIF4-*IAA19* module in a transient expression assay to evaluate the effect of phosphorylation on the function of Rht-B1b. The promoter of the PIF4 target gene *IAA19* (Sun et al. 2013) was fused to the *Luciferase* (*LUC*) gene as a reporter, followed by transient expression in *N. benthamiana* protoplasts (Fig. 4D). As expected, PIF4 activated the expression of *IAA19*$_{pro}$*:LUC*, whereas co-expression of Rht-B1b reduced the induction of *IAA19*$_{pro}$*:LUC* expression by PIF4 (Fig. 4D). Importantly, co-expression of Rht-B1b^{3A} failed to repress the PIF4-mediated induction of *IAA19*$_{pro}$*:LUC* expression (Fig. 4D), suggesting that phosphorylation by GSK3 facilitates Rht-B1b–mediated repression of target TF activity.

Finally, we compared the genome-wide gene expression profiles of *Rht-B1b-OE* and *Rht-B1b*^{3A}*-OE* transgenic wheat plants by transcriptome sequencing (RNA-seq) (Supplemental Data Sets S1 and S2). The *Rht-B1b-OE* and *Rht-B1b*^{3A}*-OE* plants displayed distinct expression patterns of cell elongation–related genes (Fig. 4E). RT-qPCR confirmed that some cell elongation–related genes were significantly downregulated in *Rht-B1b-OE* transgenic plants, while their expression appeared to be slightly reduced in *Rht-B1b*^{3A}*-OE* transgenic plants vs. wild-type Fielder (Fig. 4F).

Discussion

The growth-promoting plant hormone GA destabilizes DELLAs to promote plant growth. During the Green Revolution, the naturally N-terminally truncated DELLA proteins Rht-B1b and Rht-D1b, which are insensitive to GA-triggered degradation, were used to generate semidwarf wheat cultivars (Peng et al. 1999; Van De Velde et al. 2021). However, the underlying mechanisms of how these Green Revolution proteins reduce plant height in wheat remain unknown. Our findings, together with recent studies (Cheng et al. 2020; Gupta et al. 2021), indicate that EMS or natural mutations targeting the conserved TREE motif of GSK3 caused the dwarf wheat phenotype. Here we detected a direct interaction between GSK3 and Rht-B1b and uncovered a mechanism by which GSK3 phosphorylates the Green Revolution protein Rht-B1b (and Rht-D1b) and enhances its activity to reduce plant height, which might have contributed to the Green Revolution in wheat (Fig. 5).

The identification of phosphorylated residues is a crucial step toward understanding the relevance of phosphorylation for DELLA function. Importantly, our efforts successfully identified Ser92, Ser135, and Ser136 in the poly-Ser/Thr/Val region of the Green Revolution protein Rht-B1b as the phosphorylation sites by GSK3 (Fig. 2E). Similarly, the phosphorylation sites of rice DELLA protein SLR1 by EL1 are also located in the poly-Ser/Thr/Val domain, and the phosphorylation of SLR1 is important for maintaining its activity and stability (Dai and Xue 2010). Based on our results from observing stably transgenic wheat plants, Rht-B1b-TF interaction assays, and transient transcription activity assays, we propose that phosphorylation by GSK3 facilitates the function of Rht-B1b in repressing plant growth.

Additionally, semi-*in vivo* protein degradation assays using the fusion proteins Rht-B1b-GST and Rht-B1b^{3A}-GST showed that the protein stability of Rht-B1b^{3A}-GST was also reduced compared with stabilized Rht-B1b (Supplemental Fig. S9). Therefore, we propose that the phosphorylation of Rht-B1b by GSK3 enhances its activity and stability. In the

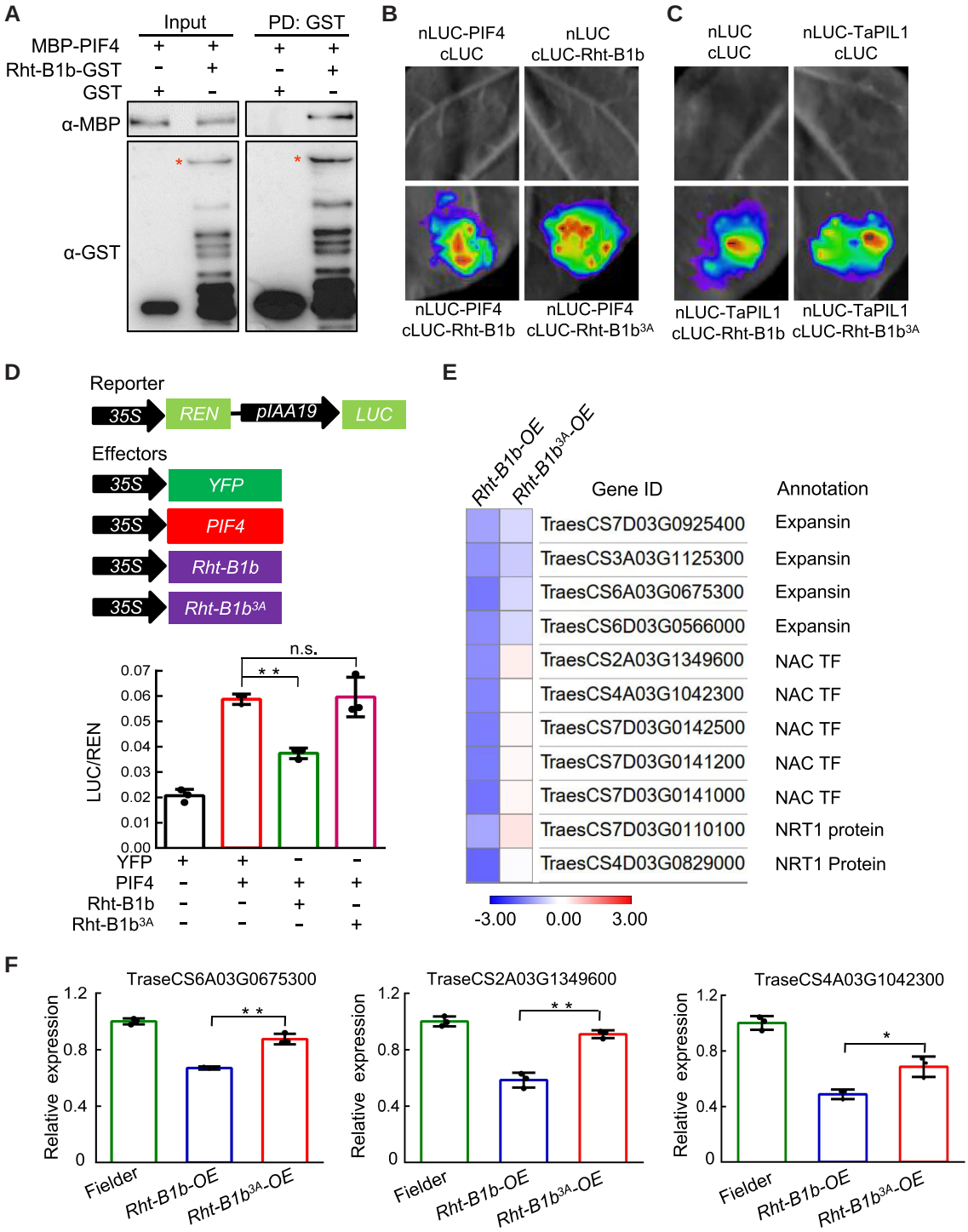

Figure 4. Phosphorylation enhances the ability of Rht-B1b to inhibit the activities of target TFs. **A)** Pull-down assay showing the in vitro interaction of Rht-B1b and PIF4. GST was used as a negative control. PD, pull down. Asterisks indicate the specific bands. **B)** LCI assay showing that Arabidopsis PIF4 interacts with Rht-B1b and Rht-B1b^{3A} in *N. benthamiana* leaves. Empty vectors were used as negative controls. **C)** LCI assay showing that wheat TaPIL1 interacts with Rht-B1b and Rht-B1b^{3A} in *N. benthamiana* leaves. Empty vectors were used as negative controls. **D)** Schematic diagrams of the reporter and effectors used in the transient transactivation assays (upper panel). Phosphorylation by GSK3 is required for Rht-B1b to repress the activity of target TFs (lower panel). *N. benthamiana* protoplasts were transfected with the reporter and different effectors. Relative LUC activities normalized to REN activity are shown (LUC/REN). Error bars represent means ± SD ($n = 3$). Asterisks indicate significant differences, and n.s. indicates no significant differences by Student's *t* test (**$P < 0.01$). **E)** Heat map of the gene expression patterns of some selected cell elongation–related genes in *Rht-B1b-OE* and *Rht-B1b^{3A}-OE* transgenic plants based on RNA-seq data. **F)** RT-qPCR analysis confirming the expression patterns of cell elongation–related genes shown in **E)**. Error bars represent means ± SD ($n = 3$). Asterisks indicate significant differences by Student's *t* test (*$0.01 < P < 0.05$ and **$P < 0.01$).

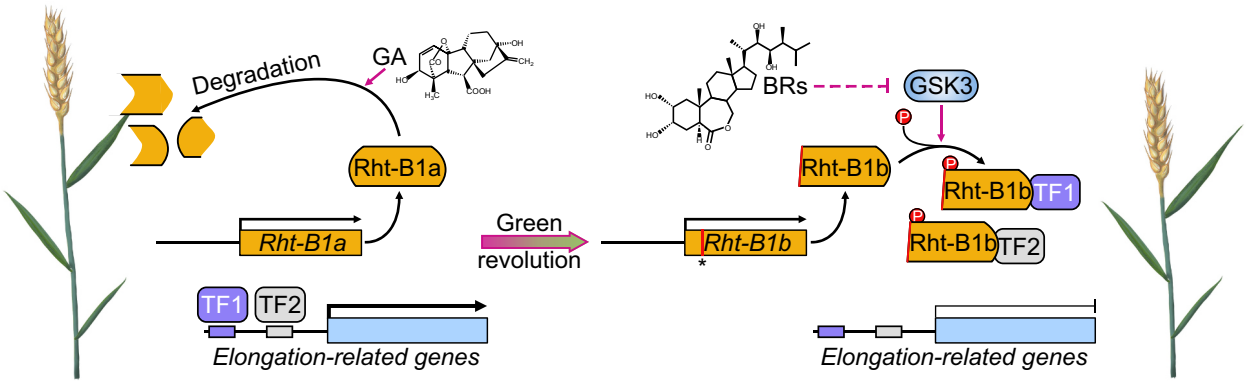

Figure 5. A proposed model of the role of GSK3 in the Green Revolution in wheat. A proposed model showing that GSK3 acts as a partner of the Green Revolution protein Rht-B1b (and Rht-D1b). Although the Rht-B1b protein derived from Rht-B1a (and Rht-D1b derived from Rht-D1a) via natural mutation became stabilized during the Green Revolution, the activity and stability of Rht-B1b (and Rht-D1b) in reducing plant height need to be facilitated by phosphorylation via GSK3. GA, gibberellin; BR, brassinosteroid; Rht-B1a, *Reduced height* (*Rht*)*-B1a*; Rht-B1b, *Reduced height* (*Rht*)*-B1b*; GSK3, glycogen synthase kinase 3; TF, transcription factor.

same manner, SUMOylation also regulates the stability and activity of DELLA proteins (Conti et al. 2014; Gonçalves et al. 2020). Interestingly, the sites of *O*-GlcNAcylation by SEC and *O*-fucosylation by SPY are also located in the nearby regions of the poly-Ser/Thr/Val domain of RGA (Zentella et al. 2016, 2017). These findings indicate that the poly-Ser/Thr/Val region at the N-termini of DELLA proteins is a site of multiple posttranslational modifications, which are vital for the functions of DELLA proteins. However, the ability of Rht-B1b^{3A} to reduce plant height was not completely abolished, suggesting that there might be other phosphorylation sites in Rht-B1b by other protein kinases. Alternatively, perhaps GSK3-induced phosphorylation is one of several mechanisms by which Rht-B1b is posttranslationally regulated. Taken together, the co-existence of multiple posttranslational modifications likely enhances the fast and flexible adjustment of DELLA function.

BR and GA are the 2 most important growth-promoting plant hormones. There is no doubt that BR and GA actively interact to regulate plant growth and development. Two independent studies reported that BR regulates plant growth by modulating GA metabolism in rice and Arabidopsis (Tong et al. 2014; Unterholzner et al. 2015). In Arabidopsis, BR and GA function interdependently via a direct interaction between the BR-activated BZR1 and GA-destructed DELLA transcriptional regulators (Bai et al. 2012). Here we revealed an additional layer of the mechanism underlying the crosstalk between BR and GA via the GSK3-DELLA module, which advances our understanding of phytohormonal crosstalk in crop plants.

Materials and methods

Plant materials and growth conditions

The wheat (*Triticum aestivum*) *gsk3* mutant was crossed with wild-type line YZ4110 to obtain the F_1 population, and the BC_4F_2 population was obtained by self-fertilization of BC_4F_1 plants. Wheat plants were grown in Beijing, China, under natural conditions or in growth chamber at 22 °C for 16 h (day, ~200 μmol m^{-2} s^{-1}, light-emitting diodes (LED) bulbs) and 18 °C for 8 h (night). *A. thaliana* ecotype Col-0 was used as the wild type. The *dellaq* (Achard et al. 2007) mutant was previously described. Arabidopsis seedlings were grown on 1/2 Murashige and Skoog (MS) medium containing 2% sucrose at 22 °C in a light incubator under a 16-h light (~100 μmol m^{-2} s^{-1}, LED bulbs)/8-h dark photoperiod. *N. benthamiana* plants were grown under a 16-h light (~120 μmol m^{-2} s^{-1}, LED bulbs)/8-h dark cycle in a greenhouse at 24 °C for 1 mo before infiltration.

Gene cloning by BSE-Seq analysis

Leaves of plants from the BC_4F_2 population were collected to construct the wild-type and mutant phenotype pools at the heading stage for genomic DNA isolation. Each pool contained 30 individuals. Genomic DNA was extracted using the cetyltriethyl ammonium bromide (CTAB) method (Saghai-Maroof et al. 1984). After quality testing, exome capture and high-throughput sequencing were conducted, which generated approximately 20 Gb of sequence data for each pool. Given the characteristics of EMS mutagenesis, certain variations were filtered out, and the candidate gene was identified by varBScore (Dong et al. 2020a).

Paraffin sections

The internodes below the spike were collected from wheat plants at the heading stage, fixed in 50% ethanol, 0.9 M glacial acetic acid, and 3.7% formaldehyde overnight at 4 °C, dehydrated in a graded ethanol series, infiltrated with xylene, and embedded in paraffin (Sigma). Eight-micrometer-thick sections were cut with a microtome (RM2245; Leica) and transferred onto poly-L-lysine–coated glass slides, deparaffinized in xylene, and dehydrated through an ethanol series

(Ma et al. 2017). Light microscopy was performed using a SteREO Discovery microscope observation system (AXIO IMAGER Z2, ZEISS).

BR treatment

Lamina inclination assays in response to BR treatment were performed as previously described (Tong et al. 2009). For the root length assays, uniform germinated seeds were selected and grown in various concentrations of epibrassinolide (eBL, an active form of BR) (Sigma, E1641-2MG) for ~7 d (22 °C/16-h light and 18 °C/8-h dark). The angles of lamina joint bending and the lengths of roots were measured using ImageJ software.

RNA extraction and RT-qPCR

Total RNAs were extracted from the samples using a Plant Total RNA Extraction kit (Zoman) according to the manufacturer's instruction. Approximately 2 μg of total RNA was used for reverse transcription with the 5× All-In One RT MasterMix system (Applied Biological Materials). The cDNA was diluted with water in a 1:5 ratio, and 2 μL diluted cDNA was used for RT-qPCR with the SYBR Premix Ex Taq Kit (TaKaRa). The PCR program comprised an initial denaturation for 1 min at 95 °C and amplification by 40 cycles of 5 s at 95 °C and 30 s at 60 °C in a StepOnePlus Real Time PCR system. All primers used for RT-qPCR are listed in Supplemental Table S2.

Generation of DNA constructs

For LCI assays, *Rht-B1a*, *Rht-B1b*, and *TaBSU1* were cloned into the *Kpn*I/*Sal*I- or *Kpn*I/*Bam*HI-digested *p1300-35S-cLUC* vector (Chen et al. 2008). Similarly, *GSK3*, *PIF4*, and *TaPIL1* were cloned into the *Kpn*I/*Sal*I-digested *p1300-35S-nLUC* vector (Chen et al. 2008). To generate the Rht-B1a-GST, Rht-B1b-GST, and Rht-B1b^{3A}-GST fusion proteins, *Rht-B1a*, *Rht-B1b*, and *Rht-B1b^{3A}* were ligated into the *Eco*RI/*Sal*I-digested *pGEX4T-1* vector (Dong et al. 2020b). To generate the MBP-GSK3 and MBP-PIF4 fusion proteins, *GSK3* and *PIF4* were ligated into the *Bam*HI/*Sal*I-digested *pMAL-c2X* vector (Dong et al. 2020b). The sequences encoding Rht-B1a and Rht-B1b were mutated to different mutant forms via nucleic acid synthesis (Tsingke) or using a Site-Directed Mutagenesis Kit (Mei5 Biotechnology, MF129-01). For the Co-IP assays, *Rht-B1b* and *GSK3* were cloned into the *Xba*I/*Bam*HI-digested *p1305-35S-GFP* (Dong et al. 2021) and *Xba*I/*Sal*I-digested *p1300-35S-Flag* vectors (Dong et al. 2021) to generate the *35S:Rht-B1b-GFP* and *35S:GSK3-Flag* constructs, respectively. All ligations were performed using the Ligation-Free Cloning Master Mix (Biomed, CL116) according to the manufacturer's instructions. The primers used to generate the DNA constructs in this study are shown in Supplemental Table S2.

Firefly LCI assays

The LCI assays to detect protein interactions were performed in *N. benthamiana* leaves as described previously (Dong et al. 2020b). Briefly, Agrobacteria harboring the indicated constructs were co-infiltrated into *N. benthamiana* leaves, and the infiltrated leaves were analyzed for LUC activity at 48 h after infiltration using a NightSHADE LB 985 in vivo plant imaging system (Berthold, Bad Wildbad, Germany).

Y2H assays

For the Y2H assays, the *Rht-B1a*, *Rht-B1b*, *Rht-B1b^{3A}*, and *GSK3* genes were cloned into the *Nde*I/*Eco*RI-digested *pGADT7* (Dong et al. 2020b) or *Nde*I/*Eco*RI enzymes digested *pGBKT7* vector (Dong et al. 2020b), respectively. These constructs were transformed into yeast (*Saccharomyces cerevisiae*) strain AH109 and grown on SD-Trp/-Leu medium. The interactions were assessed by dropping the yeast cells on SD-Trp/-Leu/-His/-Ade medium.

Protein extraction, immunoblotting, and Co-IP assays

Total proteins were extracted from the samples using extraction buffer [125 mM Tris-HCl (pH 6.8), 4% SDS, 20% glycerol, 0.001% bromophenol blue, and 2% β-mercaptoethanol]. The protein samples were boiled for 5 min and centrifuged for 10 min, and the supernatant was separated on an SDS–PAGE gel. For the immunoblotting assays, anti-Flag (1:3,000; ABclonal, AE005), anti-HA (1:2,000; Roche, 11867423001), and anti-ACT (1:5,000; CWBIO, CW0264) antibodies were used.

For the semi-in vivo protein stability assays of Rht-B1b and Rht-B1b^{3A}, the leaves of YZ4110 were collected and extracted in protein extraction buffer [50 mM Tris-MES (pH 8.0), 0.5 M sucrose, 1 mM $MgCl_2$, 10 mM EDTA, 5 mM DTT, 1 mM phenylmethylsulfonyl fluoride (PMSF), 10 μM ATP, and 1× protease inhibitor]. Approximately 5 μg of Rht-B1b-GST or Rht-B1b^{3A}-GST proteins was mixed with YZ4110 extracts and incubated for the indicated time. The samples were boiled for 5 min and analyzed by immunoblotting with anti-GST (1:3,000; CWBIO, CW0144) antibody.

For the Co-IP assays of Rht-B1b and GSK3, the Rht-B1b-GFP and GSK3-Flag proteins were transiently co-expressed in *N. benthamiana* leaves. The infiltrated leaves were collected at 48 h after infiltration and ground in liquid nitrogen, followed by protein extraction in lysis buffer [50 mM Tris-HCl (pH7.5), 150 mM NaCl, 5 mM EDTA (pH 8.0), 0.2% Triton X-100, 0.2% NP-40, 20 μM MG132, 0.6 mM PMSF, and 1× protease inhibitor]. The extracts were centrifuged at 4 °C for 20 min, and the supernatant was incubated with anti-GFP magnetic beads (MBL, D153-10) overnight. The magnetic beads were washed 5 times with lysis buffer, resuspended in 2× SDS loading buffer, and analyzed by immunoblotting with anti-GFP (1:2,000; Roche, 11814460001) and anti-Flag antibodies.

Pull-down assays

The GST, Rht-B1b-GST, MBP-GSK3, and MBP-PIF4 fusion proteins were expressed in *Escherichia coli* strain BL21. The bacterial cells were induced with 0.4 mM isopropyl β-D-1-thiogalactopyranoside (IPTG) at 18 °C for 14 h. The

GST-tagged and MBP-tagged recombinant proteins were purified using glutathione resin (GenScript) and amylose resin (NEB), respectively. For the pull-down assays of GSK3/Rht-B1b and PIF4/Rht-B1b, the indicated fusion proteins were incubated with glutathione resin for 2 h in 1× PBS buffer (CWBIO, CW0040S). The GST-bound resin was washed 5 times with 1× PBS buffer, resolved by SDS–PAGE, and detected using anti-MBP (1:3,000; CWBIO, CW0288) and anti-GST (1:3,000; CWBIO, CW0144) antibodies.

Generation of transgenic/hybrid plants

To generate *GSK3-Flag* and *gsk3-Flag* transgenic wheat plants, the coding sequences of *GSK3* and *gsk3* were cloned from wild-type YZ4110 and the *gsk3* mutant. The coding sequence of *GSK3* or *gsk3* was fused with Flag tag and subsequently ligated into the *SmaI*/*SpeI*-digested *pWMB110* vector (Liu et al. 2020). These constructs were transformed into *Agrobacterium tumefaciens* strain EHA105 and introduced into wheat cultivar KN199. To generate *Rht-B1b-OE* and *Rht-B1b*^{3A}*-OE* transgenic wheat plants, *Rht-B1b-Flag* or *Rht-B1b*^{3A}*-Flag* was ligated into the *pWMB110* vector. These constructs were transformed into *A. tumefaciens* strain EHA105 and introduced into wheat cultivar Fielder. The transgenic wheat plants were generated by an *A. tumefaciens*-mediated transformation method using the licensed protocol "PureWheat".

To generate *GSK3*^{E285K}*-Flag* transgenic wheat plants, the sequence encoding mutated GSK3^{E285K} was fused with Flag tag and subsequently ligated into the *pUbi:cas* vector (Yan et al. 2021). The *GSK3*^{E285K}*-Flag* construct was transformed into 1-mo-old embryogenic calli of KN199 by particle bombardment (Bio-Rad, Hercules, CA; Vasil and Vasil 2006).

To generate β-estradiol–inducible *pERGW-gsk3*/Col-0 and *pERGW-gsk3*/*dellaq* transgenic plants, the coding sequence of *gsk3* was ligated into the entry vector *pQBV3* (Yang et al. 2021) and then introduced into *pERGW* (Liu et al. 2017) by the Gateway cloning strategy. The binary constructs were introduced into the Col-0 or *dellaq* mutant background by *A. tumefaciens* strain GV3101–mediated transformation to generate the indicated transgenic plants (Clough and Bent 1998).

In vitro and in vivo phosphorylation assays

For the *in vitro* phosphorylation assays, 1 μg MBP-GSK3 fusion proteins were incubated with 2 μg Rht-B1a-GST/Rht-B1b-GST or mutant proteins in 20 μL kinase reaction buffer [25 mM Tris-HCl (pH7.5), 12 mM $MgCl_2$, 1 mM DTT, and 1 mM ATP] at 37 °C for 1 h. The reactions were boiled in 5× SDS loading buffer and separated by 8% SDS–PAGE in gels containing 50 μM Phos-tag (NARD, AAL-107) and 100 μM $MnCl_2$. The gel was washed 3 times using transfer buffer with 1 mM EDTA and once using transfer buffer without EDTA, each for 10 min. The gel was blotted onto a membrane and the fusion proteins were detected using anti-GST antibody.

Approximately 0.1-g leaves of transgenic wheat plants were ground in liquid nitrogen and incubated in 300 μL extraction buffer (150 mM KCl, 50 mM HEPES, 1 mM DTT, 0.4% Triton X-100, 1× protein inhibitor, and 1× Phostop) for 30 min on ice. The extracts were centrifuged at 4 °C for 30 min, and the supernatant was mixed with 5× SDS loading buffer. After boiling for 5 min, the samples were separated by 8% SDS–PAGE in a gel containing 50 μM Phos-tag and 100 μM $MnCl_2$.

Mass spectrometry

To prepare samples for mass spectrometry, 10 μg Rht-B1b-GST and 5 μg MBP-GSK3 recombinant proteins were incubated in 100 μL kinase reaction buffer at 37 °C for 1 h. The reactions were boiled in 5× SDS loading buffer and separated by 8% SDS–PAGE in a gel containing 50 μM Phos-tag and 100 μM $MnCl_2$. The in-gel proteins were reduced with dithiothreitol (10 mM DTT/100 mM NH_4HCO_3) and alkylated with iodoacetamide (200 mM IAA/100 mM NH_4HCO_3). LC-MS/MS analysis was performed on a Q Exactive mass spectrometer (Thermo Fisher Scientific) coupled to an Easy-nLC liquid chromatography system (Thermo Fisher Scientific). For protein identification, the following options were used: peptide mass tolerance: 20 ppm; fragment mass tolerance: 0.1 Da; enzyme: trypsin; missed cleavage: 2; fixed modification: carbamidomethyl (C); and variable modification: Phospho (STY).

RNA sequencing and data analysis

The coleoptiles of Fielder, *Rht-B1b-OE*, and *Rht-B1b*^{3A}*-OE* plants were collected at the 1-leaf stage, and total RNA was extracted from the samples using TRIzol reagent (Invitrogen) according to the manufacturer's instructions. For each genotype plant, 5 coleoptiles were collected to extract RNA, and 3 biological replicates were employed. cDNA libraries were generated and sequenced on the Illumina NovaSeq 6000 platform (Illumina Inc., USA) to generate more than 10 Gb raw data for each library. The raw reads were cleaned to remove low-quality reads and adapters with Fastp (v0.12.4). The RNA-seq reads were mapped to the reference genome IWGSC RefSeq v2.1 using HISAT2. Differential expression analysis was performed using the DESeq2 (1.34.0) package in R. Differentially expressed genes (DEGs) were identified with $\log_2$ (fold change) ≥ 1 and $P < 0.05$. Morpheus (https://software.broadinstitute.org/morpheus) was used to construct heat maps.

Transient transcription dual-luciferase assays

The promoter of *IAA19* (1,907 bp) was cloned into the *KpnI*/*BamHI*-digested *pGreenII 0800-LUC* vector (Yang et al. 2021) as a reporter. The *REN* gene under the control of the cauliflower mosaic virus *35S* promoter in the *pGreenII 0800-LUC* vector was used as the internal control. *PIF4*, *Rht-B1b*, and *Rht-B1b*^{3A} were cloned into the *p2GW7* (Yang et al. 2021) vector by the Gateway cloning strategy as effectors. Transient transcription dual-luciferase (dual-LUC) assays

were performed in *N. benthamiana* protoplasts isolated from 3- to 4-wk-old plants grown under long-day conditions (16-h light/8-h dark) as described previously (Yoo et al. 2007). The protoplasts were transfected with a total of 15 μg DNA and incubated in the dark for 18 h. The luciferase activity of these protoplasts was analyzed using the Dual-Luciferase Reporter system (Promega, E1910) according to the manufacturer's instruction.

Statistical analysis

All statistics were calculated using the SPSS Statistics software. To determine statistical significance, we employed Student' with Dunnett's multiple comparison test. A value of $P < 0.05$ was considered to indicate statistical significance. All sample sizes and significance thresholds are indicated in the figure legends. Student' Supplemental Tables S3 and S4, respectively.

Accession numbers

Wheat and Arabidopsis gene sequence data from this study can be found in the Ensembl Plants data library under the following accession numbers: Rht-B1, TraesCS4B02G043100; TaGSK3, TraesCS3D02G137200; TaPIL1-5A, TraesCS5A02G376500; TaPIL1-5B, TraesCS5B02G380200; TaPIL1-5D, TraesCS5D02G386500; TaBSU1-1B, TraesCS1B02G107000; BIN2, At4G18710; PIF4, At2G43010; and IAA19, At3G15540.

Author contributions

J.S. and X.K. conceived this project; J.S. designed the research; H.D., D.L., R.Y., L.Z., and Y.Z. performed the experiments; H.D. and D.L. wrote the manuscript; J.S. and X.K. revised the manuscript; X.L. supervised this research.

Supplemental data

The following materials are available in the online version of this article.

Supplemental Figure S1. Phenotypes of the gain-of-function mutant *gsk3* (supports Fig. 1).

Supplemental Figure S2. BR-insensitive phenotypes of the gain-of-function mutant *gsk3* (supports Fig. 1).

Supplemental Figure S3. Cloning of the *gsk3* gene (supports Fig. 1).

Supplemental Figure S4. Protein sequence alignment showing the Glu286Lys point mutation in gsk3 mutant protein (supports Fig. 1).

Supplemental Figure S5. GSK3 interacts with TaBSU1 (supports Fig. 1).

Supplemental Figure S6. Phosphorylation sites of Rht-1 by GSK3 (supports Fig. 2).

Supplemental Figure S7. Identification of phosphopeptides of Rht-B1b by LC-MS/MS (supports Fig. 2).

Supplemental Figure S8. Phenotypes of *pERGW-gsk3*/Col-0 and *pERGW-gsk3/dellaq* transgenic Arabidopsis plants (supports Fig. 3).

Supplemental Figure S9. Degradation rates of Rht-B1b and Rht-B1b^{3A} in cell-free assays from YZ4110 protein extracts (supports Fig. 4).

Supplemental Table S1. Plant height of *Rht-OE* transgenic wheat lines.

Supplemental Table S2. Constructs and primers used in this study.

Supplemental Table S3. Results of Student's *t* test in this study.

Supplemental Table S4. Results of ANOVA with Dunnett's multiple comparisons test in this study.

Supplemental Data Set S1. Differentially expressed genes between *Rht-B1b-OE* and Fielder.

Supplemental Data Set S2. Differentially expressed genes between *Rht-B1b^{3A}-OE* and Fielder.

Funding

This work was supported by the National Natural Science Foundation of China (31971880 and 91935304), the Central Public-interest Scientific Institution Basal Research Fund (S2022ZD02), and the Agricultural Science and Technology Innovation Program of CAAS.

Conflict of interest statement. None declared.

Data availability

The RNA sequencing data have been deposited in the National Center for Biotechnology Information (NCBI): accession number PRJNA943387.

References

Achard P, Liao L, Jiang C, Desnos T, Bartlett J, Fu X, Harberd NP. DELLAs contribute to plant photomorphogenesis. Plant Physiol. 2007:**143**(3):1163–1172. https://doi.org/10.1104/pp.106.092254

Bai MY, Shang JX, Oh E, Fan M, Bai Y, Zentella R, Sun TP, Wang ZY. Brassinosteroid, gibberellin and phytochrome impinge on a common transcription module in *Arabidopsis*. Nat Cell Biol. 2012:**14**(8):810–817. https://doi.org/10.1038/ncb2546

Blanco-Tourinan N, Legris M, Minguet EG, Costigliolo-Rojas C, Nohales MA, Iniesto E, Garcia-Leomicronn M, Pacin M, Heucken N, Blomeier T, et al. COP1 destabilizes DELLA proteins in *Arabidopsis*. Proc Natl Acad Sci USA. 2020a:**117**(24):13792–13799. https://doi.org/10.1073/pnas.1907969117

Blanco-Tourinan N, Serrano-Mislata A, Alabadi D. Regulation of DELLA proteins by post-translational modifications. Plant Cell Physiol. 2020b:**61**(11):1891–1901. https://doi.org/10.1093/pcp/pcaa113

Chen H, Zou Y, Shang Y, Lin H, Wang Y, Cai R, Tang X, Zhou JM. Firefly luciferase complementation imaging assay for protein-protein interactions in plants. Plant Physiol. 2008:**146**(2):323–324. https://doi.org/10.1104/pp.107.111740

Cheng X, Xin M, Xu R, Chen Z, Cai W, Chai L, Xu H, Jia L, Feng Z, Wang Z, et al. A single amino acid substitution in STKc_GSK3 kinase conferring semispherical grains and its implications for the origin of *Triticum sphaerococcum* Perc. Plant Cell. 2020:**32**(4):923–934. https://doi.org/10.1105/tpc.19.00580

Clough SJ, Bent AF. Floral dip: a simplified method for Agrobacterium-mediated transformation of *Arabidopsis thaliana*.

Plant J. 1998:**16**(6):735–743. https://doi.org/10.1046/j.1365-313x.1998.00343.x

Conti L, Nelis S, Zhang C, Woodcock A, Swarup R, Galbiati M, Tonelli C, Napier R, Hedden P, Bennett M, et al. Small ubiquitin-like modifier protein SUMO enables plants to control growth independently of the phytohormone gibberellin. Dev Cell. 2014:**28**(1):102–110. https://doi.org/10.1016/j.devcel.2013.12.004

Dai C, Xue HW. Rice early flowering1, a CKI, phosphorylates DELLA protein SLR1 to negatively regulate gibberellin signalling. EMBO J. 2010:**29**(11):1916–1927. https://doi.org/10.1038/emboj.2010.75

de Lucas M, Daviere JM, Rodriguez-Falcon M, Pontin M, Iglesias-Pedraz JM, Lorrain S, Fankhauser C, Blazquez MA, Titarenko E, Prat S. A molecular framework for light and gibberellin control of cell elongation. Nature. 2008:**451**(7177):480–484. https://doi.org/10.1038/nature06520

Dill A, Thomas SG, Hu J, Steber CM, Sun TP. The *Arabidopsis* F-box protein SLEEPY1 targets gibberellin signaling repressors for gibberellin-induced degradation. Plant Cell. 2004:**16**(6):1392–1405. https://doi.org/10.1105/tpc.020958

Dong H, Liu J, He G, Liu P, Sun J. Photoexcited phytochrome B interacts with brassinazole resistant 1 to repress brassinosteroid signaling in *Arabidopsis*. J Integr Plant Biol. 2020b:**62**(5):652–667. https://doi.org/10.1111/jipb.12822

Dong H, Yan S, Jing Y, Yang R, Zhang Y, Zhou Y, Zhu Y, Sun J. MIR156-targeted SPL9 is phosphorylated by SnRK2s and interacts with ABI5 to enhance ABA responses in *Arabidopsis*. Front Plant Sci. 2021:**12**:708573. https://doi.org/10.3389/fpls.2021.708573

Dong C, Zhang L, Chen Z, Xia C, Gu Y, Wang J, Li D, Xie Z, Zhang Q, Zhang X, et al. Combining a new exome capture panel with an effective varBScore algorithm accelerates BSA-based gene cloning in wheat. Front Plant Sci. 2020a:**11**:1249. https://doi.org/10.3389/fpls.2020.01249

Feng S, Martinez C, Gusmaroli G, Wang Y, Zhou J, Wang F, Chen L, Yu L, Iglesias-Pedraz JM, Kircher S, et al. Coordinated regulation of *Arabidopsis thaliana* development by light and gibberellins. Nature. 2008:**451**(7177):475–479. https://doi.org/10.1038/nature06448

Gonçalves NM, Fernandes T, Nunes C, Rosa MTG, Matiolli CC, Rodrigues MAA, Barros PM, Oliveira MM, Abreu IA. SUMOylation of rice DELLA SLR1 modulates transcriptional responses and improves yield under salt stress. bioRxiv. 10.1101/2020.03.10.986224, 12 May 2020, preprint: not peer reviewed.

Gupta A, Hua L, Lin G, Molnar I, Dolezel J, Liu S, Li W. Multiple origins of Indian dwarf wheat by mutations targeting the TREE domain of a GSK3-like kinase for drought tolerance, phosphate uptake, and grain quality. Theor Appl Genet. 2021:**134**(2):633–645. https://doi.org/10.1007/s00122-020-03719-5

Harberd NP, Belfield E, Yasumura Y. The angiosperm gibberellin-GID1-DELLA growth regulatory mechanism: how an "inhibitor of an inhibitor" enables flexible response to fluctuating environments. Plant Cell. 2009:**21**(5):1328–1339. https://doi.org/10.1105/tpc.109.066969

He JX, Gendron JM, Yang Y, Li J, Wang ZY. The GSK3-likea kinase BIN2 phosphorylates and destabilizes BZR1, a positive regulator of the brassinosteroid signaling pathway in *Arabidopsis*. Proc Natl Acad Sci USA. 2002:**99**(15):10185–10190. https://doi.org/10.1073/pnas.152342599

Hirano K, Asano K, Tsuji H, Kawamura M, Mori H, Kitano H, Ueguchi-Tanaka M, Matsuoka M. Characterization of the molecular mechanism underlying gibberellin perception complex formation in rice. Plant Cell. 2010:**22**(8):2680–2696. https://doi.org/10.1105/tpc.110.075549

Li J, Nam KH. Regulation of brassinosteroid signaling by a GSK3/SHAGGY-like kinase. Science. 2002:**295**(5558):1299–1301. https://doi.org/10.1126/science.1065769

Li J, Nam KH, Vafeados D, Chory J. BIN2, a new brassinosteroid-insensitive locus in *Arabidopsis*. Plant Physiol. 2001:**127**(1):14–22. https://doi.org/10.1104/pp.127.1.14

Liu J, Cheng X, Liu P, Li D, Chen T, Gu X, Sun J. MicroRNA319-regulated TCPs interact with FBHs and PFT1 to activate *CO* transcription and control flowering time in *Arabidopsis*. PLoS Genet. 2017:**13**(5):e1006833. https://doi.org/10.1371/journal.pgen.1006833

Liu H, Wang K, Tang H, Gong Q, Du L, Pei X, Ye X. CRISPR/Cas9 editing of wheat *TaQ* genes alters spike morphogenesis and grain threshability. J Genet Genomics. 2020:**47**(9):563–575. https://doi.org/10.1016/j.jgg.2020.08.004

Ma L, Sang X, Zhang T, Yu Z, Li Y, Zhao F, Wang Z, Wang Y, Yu P, Wang N, et al. ABNORMAL VASCULAR BUNDLES regulates cell proliferation and procambium cell establishment during aerial organ development in rice. New Phytol. 2017:**213**(1):275–286. https://doi.org/10.1111/nph.14142

Murase K, Hirano Y, Sun TP, Hakoshima T. Gibberellin-induced DELLA recognition by the gibberellin receptor GID1. Nature. 2008:**456**(7221):459–463. https://doi.org/10.1038/nature07519

Peng J, Richards DE, Hartley NM, Murphy GP, Devos KM, Flintham JE, Beales J, Fish LJ, Worland AJ, Pelica F, et al. 'Green revolution' genes encode mutant gibberellin response modulators. Nature. 1999:**400**(6741):256–261. https://doi.org/10.1038/22307

Qin Q, Wang W, Guo X, Yue J, Huang Y, Xu X, Li J, Hou S. *Arabidopsis* DELLA protein degradation is controlled by a type-one protein phosphatase, TOPP4. PLoS Genet. 2014:**10**(7):e1004464. https://doi.org/10.1371/journal.pgen.1004464

Saghai-Maroof MA, Soliman KM, Jorgensen RA, Allard RW. Ribosomal DNA spacer-length polymorphisms in barley: Mendelian inheritance, chromosomal location, and population dynamics. Proc Natl Acad Sci USA. 1984:**81**(24):8014–8018. https://doi.org/10.1073/pnas.81.24.8014

Sasaki A, Itoh H, Gomi K, Ueguchi-Tanaka M, Ishiyama K, Kobayashi M, Jeong DH, An G, Kitano H, Ashikari M, et al. Accumulation of phosphorylated repressor for gibberellin signaling in an F-box mutant. Science. 2003:**299**(5614):1896–1898. https://doi.org/10.1126/science.1081077

Sun J, Qi L, Li Y, Zhai Q, Li C. PIF4 and PIF5 transcription factors link blue light and auxin to regulate the phototropic response in *Arabidopsis*. Plant Cell. 2013:**25**(6):2102–2114. https://doi.org/10.1105/tpc.113.112417

Tong H, Chu C. Functional specificities of brassinosteroid and potential utilization for crop improvement. Trends Plant Sci. 2018:**23**(11):1016–1028. https://doi.org/10.1016/j.tplants.2018.08.007

Tong H, Jin Y, Liu W, Li F, Fang J, Yin Y, Qian Q, Zhu L, Chu C. DWARF AND LOW-TILLERING, a new member of the GRAS family, plays positive roles in brassinosteroid signaling in rice. Plant J. 2009:**58**(5):803–816. https://doi.org/10.1111/j.1365-313X.2009.03825.x

Tong H, Xiao Y, Liu D, Gao S, Liu L, Yin Y, Jin Y, Qian Q, Chu C. Brassinosteroid regulates cell elongation by modulating gibberellin metabolism in rice. Plant Cell. 2014:**26**(11):4376–4393. https://doi.org/10.1105/tpc.114.132092

Ueguchi-Tanaka M, Ashikari M, Nakajima M, Itoh H, Katoh E, Kobayashi M, Chow TY, Hsing YI, Kitano H, Yamaguchi I, et al. GIBBERELLIN INSENSITIVE DWARF1 encodes a soluble receptor for gibberellin. Nature. 2005:**437**(7059):693–698. https://doi.org/10.1038/nature04028

Unterholzner SJ, Rozhon W, Papacek M, Ciomas J, Lange T, Kugler KG, Mayer KF, Sieberer T, Poppenberger B. Brassinosteroids are master regulators of gibberellin biosynthesis in *Arabidopsis*. Plant Cell. 2015:**27**(8):2261–2272. https://doi.org/10.1105/tpc.15.00433

Van De Velde K, Thomas SG, Heyse F, Kaspar R, Van Der Straeten D, Rohde A. N-terminal truncated RHT-1 proteins generated by translational reinitiation cause semi-dwarfing of wheat Green Revolution alleles. Mol Plant. 2021:**14**(4):679–687. https://doi.org/10.1016/j.molp.2021.01.002

Vasil IK, Vasil V. Transformation of wheat via particle bombardment. Methods Mol Biol. 2006:**318**:273–283. https://doi.org/10.1385/1-59259-959-1:273

Wang ZY, Nakano T, Gendron J, He J, Chen M, Vafeados D, Yang Y, Fujioka S, Yoshida S, Asami T, et al. Nuclear-localized BZR1

mediates brassinosteroid-induced growth and feedback suppression of brassinosteroid biosynthesis. Dev Cell. 2002:**2**(4):505–513. https://doi.org/10.1016/S1534-5807(02)00153-3

Yan J, Li X, Zeng B, Zhong M, Yang J, Yang P, Li X, He C, Lin J, Liu X, et al. FKF1 F-box protein promotes flowering in part by negatively regulating DELLA protein stability under long-day photoperiod in *Arabidopsis*. J Integr Plant Biol. 2020:**62**(11):1717–1740. https://doi.org/10.1111/jipb.12971

Yan B, Yang Z, He G, Jing Y, Dong H, Ju L, Zhang Y, Zhu Y, Zhou Y, Sun J. The blue light receptor CRY1 interacts with GID1 and DELLA proteins to repress gibberellin signaling and plant growth. Plant Commun. 2021:**2**(6):100245. https://doi.org/10.1016/j.xplc.2021.100245

Yang Z, Yan B, Dong H, He G, Zhou Y, Sun J. BIC1 acts as a transcriptional coactivator to promote brassinosteroid signaling and plant growth. EMBO J. 2021:**40**(1):e104615. https://doi.org/10.15252/embj.2020104615

Yin Y, Wang ZY, Mora-Garcia S, Li J, Yoshida S, Asami T, Chory J. BES1 accumulates in the nucleus in response to brassinosteroids to regulate gene expression and promote stem elongation. Cell. 2002:**109**(2):181–191. https://doi.org/10.1016/S0092-8674(02)00721-3

Yoo SD, Cho YH, Sheen J. *Arabidopsis* mesophyll protoplasts: a versatile cell system for transient gene expression analysis. Nat Protoc. 2007:**2**(7):1565–1572. https://doi.org/10.1038/nprot.2007.199

Youn JH, Kim TW. Functional insights of plant GSK3-like kinases: multi-taskers in diverse cellular signal transduction pathways. Mol Plant. 2015:**8**(4):552–565. https://doi.org/10.1016/j.molp.2014.12.006

Yu X, Li L, Zola J, Aluru M, Ye H, Foudree A, Guo H, Anderson S, Aluru S, Liu P, et al. A brassinosteroid transcriptional network revealed by genome-wide identification of BESI target genes in *Arabidopsis thaliana*. Plant J. 2011:**65**(4):634–646. https://doi.org/10.1111/j.1365-313X.2010.04449.x

Zentella R, Hu J, Hsieh WP, Matsumoto PA, Dawdy A, Barnhill B, Oldenhof H, Hartweck LM, Maitra S, Thomas SG, et al. O-GlcNAcylation of master growth repressor DELLA by SECRET AGENT modulates multiple signaling pathways in *Arabidopsis*. Genes Dev. 2016:**30**(2):164–176. https://doi.org/10.1101/gad.270587.115

Zentella R, Sui N, Barnhill B, Hsieh WP, Hu J, Shabanowitz J, Boyce M, Olszewski NE, Zhou P, Hunt DF, et al. The *Arabidopsis* O-fucosyltransferase SPINDLY activates nuclear growth repressor DELLA. Nat Chem Biol. 2017:**13**(5):479–485. https://doi.org/10.1038/nchembio.2320

Zhang L, He G, Li Y, Yang Z, Liu T, Xie X, Kong X, Sun J. PIL transcription factors directly interact with SPLs and repress tillering/branching in plants. New Phytol. 2022:**233**(3):1414–1425. https://doi.org/10.1111/nph.17872